Solvation-Solvophobicity Interplay Drives Reentrant Swelling of Polymer in Solvent Mixtures

Chinmoy Saha[1,2], Xiangyu Zhang[3], Md Masrul Huda[2], Neeraj Rai[2,†], and Dong Meng[1,*]

[1]Biomaterials Division, Department of Molecular Pathobiology, New York University, New York, USA

[2]Dave C. Swalm School of Chemical Engineering, and Center for Advanced Vehicular System, Mississippi State University, Mississippi State, MS-39762, USA

[3]Department of Chemical Engineering, Johns Hopkins University, Maryland, USA

[†]neerajrai@che.msstate.edu

[*]dm173@nyu.edu

July 23, 2025

Supplementary Information

Volume fraction- vs. Molar fraction-based Linear Interpolation Density

Consider a binary mixture composed of components S and C of a total volume of V. The volume fraction-based linear interpolation density of the mixture is defined as $\rho^V \equiv y_{\mathrm{C}}\rho_{\mathrm{C}} + y_{\mathrm{S}}\rho_{\mathrm{S}}$ where $\rho_\alpha = \frac{M_\alpha}{v_\alpha}$ is the mass density of component α, with M_α and v_α denoting the molar mass and molar volume of component α, respectively. The volume fraction of component α is defined as $y_\alpha \equiv \frac{n_\alpha v_\alpha}{\sum_{\alpha=S,C} n_\alpha v_\alpha}$, where n_α is the number of moles of component α in the mixture. The relation between ρ^V and true density of the mixture $\rho = \frac{n_{\mathrm{C}}M_{\mathrm{C}}+n_{\mathrm{S}}M_{\mathrm{S}}}{V}$ can be derived as:

$$
\begin{aligned}
\rho^V &= y_{\mathrm{C}}\rho_{\mathrm{C}} + y_{\mathrm{S}}\rho_{\mathrm{S}} \\
&= \frac{n_{\mathrm{C}}v_{\mathrm{C}}\rho_{\mathrm{C}}}{n_{\mathrm{C}}v_{\mathrm{C}} + n_{\mathrm{S}}v_{\mathrm{S}}} + \frac{n_{\mathrm{S}}v_{\mathrm{S}}\rho_{\mathrm{S}}}{n_{\mathrm{C}}v_{\mathrm{C}} + n_{\mathrm{S}}v_{\mathrm{S}}} \\
&= \frac{n_{\mathrm{C}}v_{\mathrm{C}}\frac{M_{\mathrm{C}}}{v_{\mathrm{C}}}}{n_{\mathrm{C}}v_{\mathrm{C}} + n_{\mathrm{S}}v_{\mathrm{S}}} + \frac{n_{\mathrm{S}}v_{\mathrm{S}}\frac{M_{\mathrm{S}}}{v_{\mathrm{S}}}}{n_{\mathrm{C}}v_{\mathrm{C}} + n_{\mathrm{S}}v_{\mathrm{S}}} \\
&= \frac{n_{\mathrm{C}}M_{\mathrm{C}}}{n_{\mathrm{C}}v_{\mathrm{C}} + n_{\mathrm{S}}v_{\mathrm{S}}} + \frac{n_{\mathrm{S}}M_{\mathrm{S}}}{n_{\mathrm{C}}v_{\mathrm{C}} + n_{\mathrm{S}}v_{\mathrm{S}}} \\
&= \frac{n_{\mathrm{C}}M_{\mathrm{C}} + n_{\mathrm{S}}M_{\mathrm{S}}}{n_{\mathrm{C}}v_{\mathrm{C}} + n_{\mathrm{S}}v_{\mathrm{S}}} \\
&= \frac{n_{\mathrm{C}}M_{\mathrm{C}} + n_{\mathrm{S}}M_{\mathrm{S}}}{V_0} \\
&= \frac{n_{\mathrm{C}}M_{\mathrm{C}} + n_{\mathrm{S}}M_{\mathrm{S}}}{V - V^E}
\end{aligned}
$$

where $V_0 \equiv n_{\mathrm{C}}v_{\mathrm{C}} + n_{\mathrm{S}}v_{\mathrm{S}}$ is the sum of component volume before mixing, and $V^E \equiv V - V_0$ denotes the excess volume of mixing. Therefore, $\frac{1}{\rho^V} = \frac{1}{\rho} - \frac{V^E}{n_{\mathrm{C}}M_{\mathrm{C}}+n_{\mathrm{S}}M_{\mathrm{S}}}$. In another word, ρ^V recovers the true volume of the mixture if the excess volume of mixing is zero. For $\rho > \rho^V$, as is the case for the mixtures of water and t-BuOH (see Figure 1(c)), there is $V^E < 0$ which means that the solution mixture becomes more "crowded" upon mixing.

On the other hand, the molar fraction-based linear interpolation density of the mixture is defined as $\rho^M \equiv x_{\mathrm{C}}\rho_{\mathrm{C}} + x_{\mathrm{S}}\rho_{\mathrm{S}}$, with $x_\alpha \equiv \frac{n_\alpha}{\sum_{\alpha=S,C} n_\alpha}$. Difference between ρ^M and ρ is given by

$$
\begin{aligned}
\rho - \rho^M &= \frac{n_{\mathrm{C}}M_{\mathrm{C}} + n_{\mathrm{S}}M_{\mathrm{S}}}{V} - \left(\frac{n_{\mathrm{C}}}{n_{\mathrm{C}} + n_{\mathrm{S}}}\frac{M_{\mathrm{C}}}{v_{\mathrm{C}}} + \frac{n_{\mathrm{S}}}{n_{\mathrm{C}} + n_{\mathrm{S}}}\frac{M_{\mathrm{S}}}{v_{\mathrm{S}}}\right) \\
&= n_{\mathrm{C}}M_{\mathrm{C}}\left(\frac{1}{n_{\mathrm{C}}v_{\mathrm{C}} + n_{\mathrm{S}}v_{\mathrm{S}} + V^E} - \frac{1}{n_{\mathrm{C}}v_{\mathrm{C}} + n_{\mathrm{S}}v_{\mathrm{C}}}\right) \\
&+ n_{\mathrm{S}}M_{\mathrm{S}}\left(\frac{1}{n_{\mathrm{C}}v_{\mathrm{C}} + n_{\mathrm{S}}v_{\mathrm{S}} + V^E} - \frac{1}{n_{\mathrm{C}}v_{\mathrm{S}} + n_{\mathrm{S}}v_{\mathrm{S}}}\right)
\end{aligned}
$$

For $\rho < \rho^M$, as is the case for the mixtures of water and t-BuOH (see Figure 1(b)), the sign of V^E cannot be directly determined. In other words, the molar fraction-based linear interpolation density, ρ^M, does not reliably indicate whether the mixture becomes more or less crowded upon mixing.

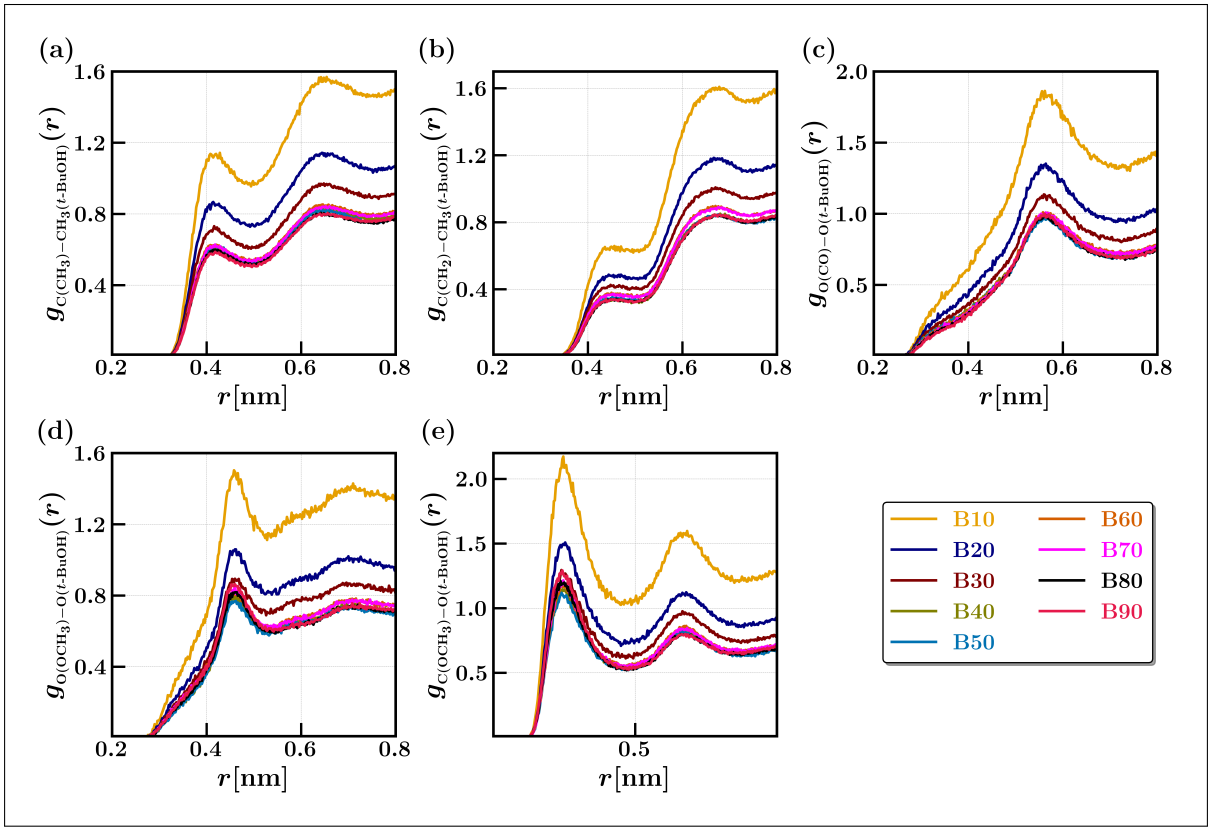

Figure S1: Radial distribution functions, $g(r)$, t-BuOH relative to various functional groups of the polymer: (a) methyl carbon [$C(CH_3)$] of t-BuOH with pendant methyl groups [$C(CH_3)$] of the polymer; (b) methyl carbon of t-BuOH with backbone methylene groups [$C(CH_2)$] of the polymer; (c) oxygen of t-BuOH with carbonyl oxygen atoms [O(CO)]; (d) oxygen of t-BuOH with methoxy oxygen atoms [$O(OCH_3)$]; and (e) oxygen of t-BuOH with methoxy carbon atoms [$C(OCH_3)$].

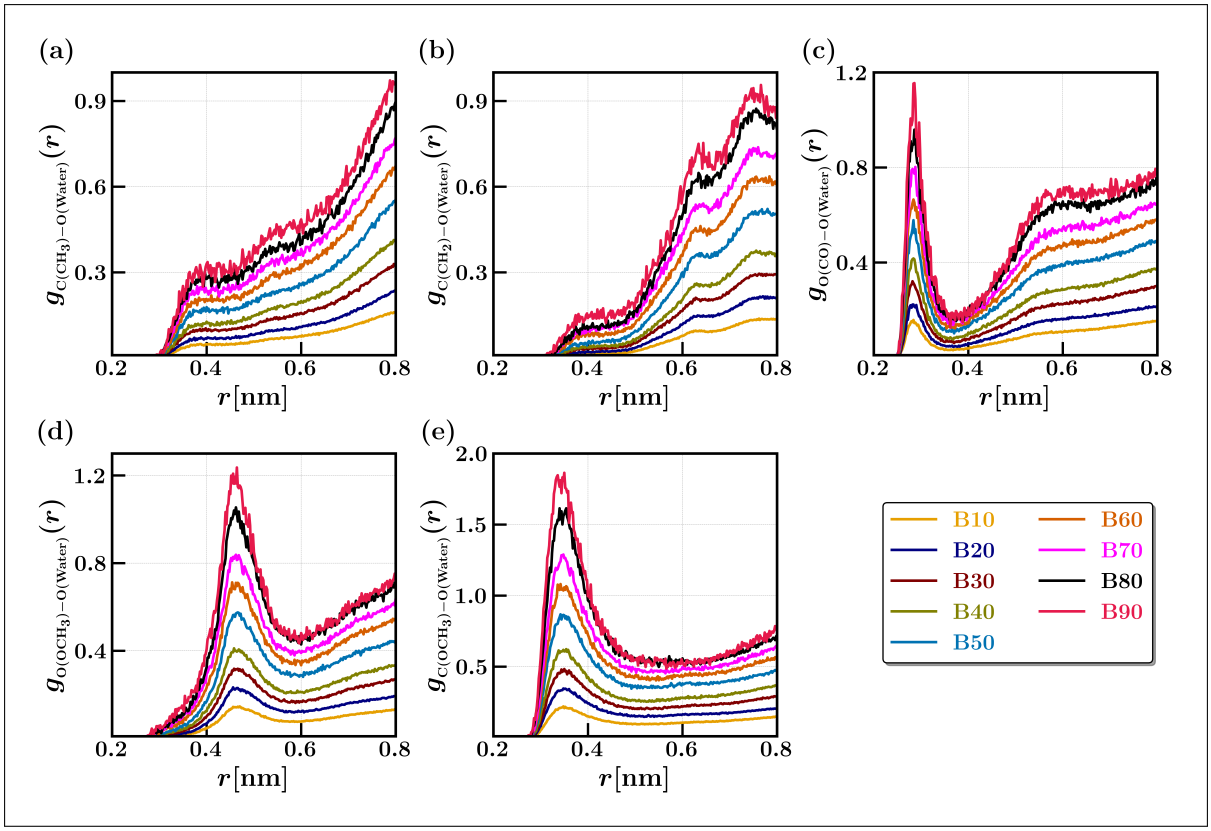

Figure S2: Radial distribution functions, $g(r)$, of the oxygen atom of water molecules with respect to various functional groups of the polymer: (a) pendant methyl carbon atoms [$C(CH_3)$]; (b) backbone methylene carbon atoms [$C(CH_2)$]; (c) carbonyl oxygen atoms [O(CO)]; (d) methoxy oxygen atoms [$O(OCH_3)$]; and (e) methoxy carbon atoms [$C(OCH_3)$].

It should be noted that Figures S1(d) and S2(d) do not represent independent molecular distributions. The $O(OCH_3)$ site includes contributions from the same *t*-BuOH or water molecules that are already counted in the distributions for the O(CO) and $C(OCH_3)$ sites, as shown in Figures S1(c,e) and S2(c,e). Based on radial distribution function (RDF) analyses (Figures S1 and S2), the site-specific interactions between various functional groups of PMMA and t-BuOH or water molecules occur predominantly within 0.35 nm. Accordingly, this distance is defined as the first solvation shell (FSS). The number of *t*-BuOH or water molecules, n_α^s, within the FSS is calculated by counting all molecules located within 0.35 nm of any atom of the PMMA chain. In contrast, to determine the number of solvent molecules, n_α^c, in contact with a specific site of PMMA, the cutoff distance is set to the position of the first peak observed in the corresponding RDF (Figure S1 ans S2). In addition, the water and *t*-BuOH molecules attracted to the methoxy carbon atoms [$C(OCH_3)$] due to partial positive charge (+0.16 e)on the C atom and negative charge on O atoms of water and *t*-BuOH, as observed in Figure S1(e) and S2(e).

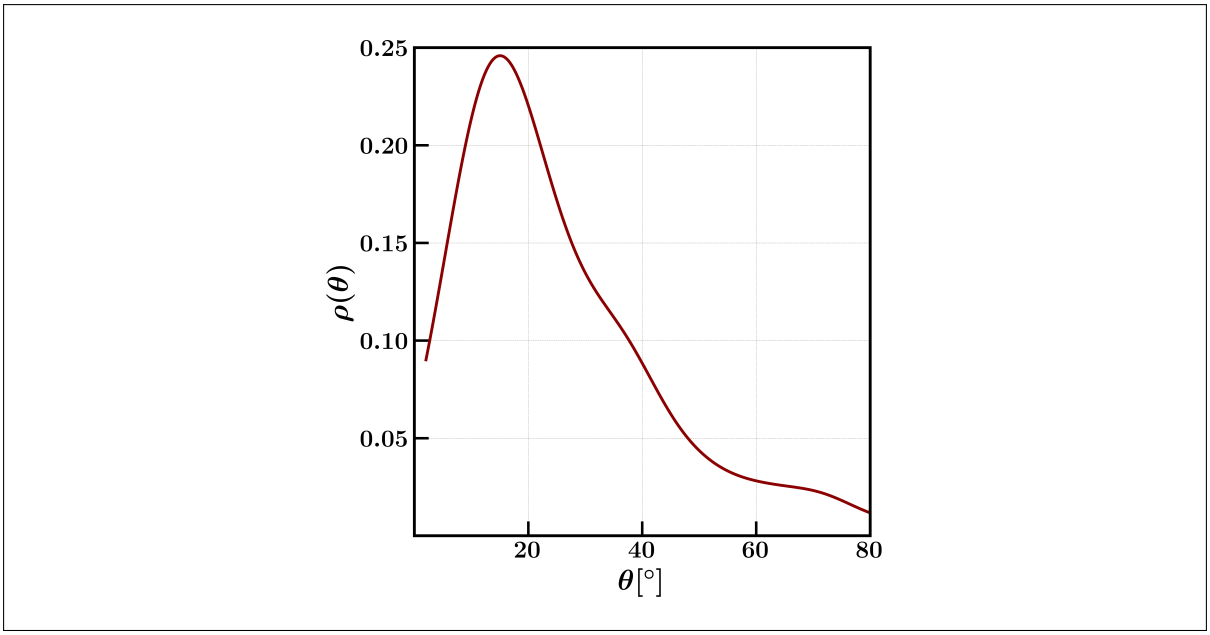

Figure S3: The normalized angular distribution ($\rho(r)$), expressed as the ratio of observations $\frac{N(\theta)}{N_{\text{total}}}$, plotted as a function of angle (θ). Here, $N(\theta)$ denotes the numer of observations at a specific angle, and N_{total} is the total number of observations.

The angle distribution presented here includes only those water molecules located within 0.35 nm of the carbonyl oxygen (O(CO)) atoms of PMMA. The distribution further confirms that the hydrogen bonding (H-bond) criteria employed in this study encompass the majority of water molecules within this distance. Specifically, a hydrogen bond is considered to be formed when the oxygen–oxygen ($\text{O}\cdots\text{O}$) distance is ≤ 0.35 nm and the $\angle$ O-O-H $\leq 0.30°$.

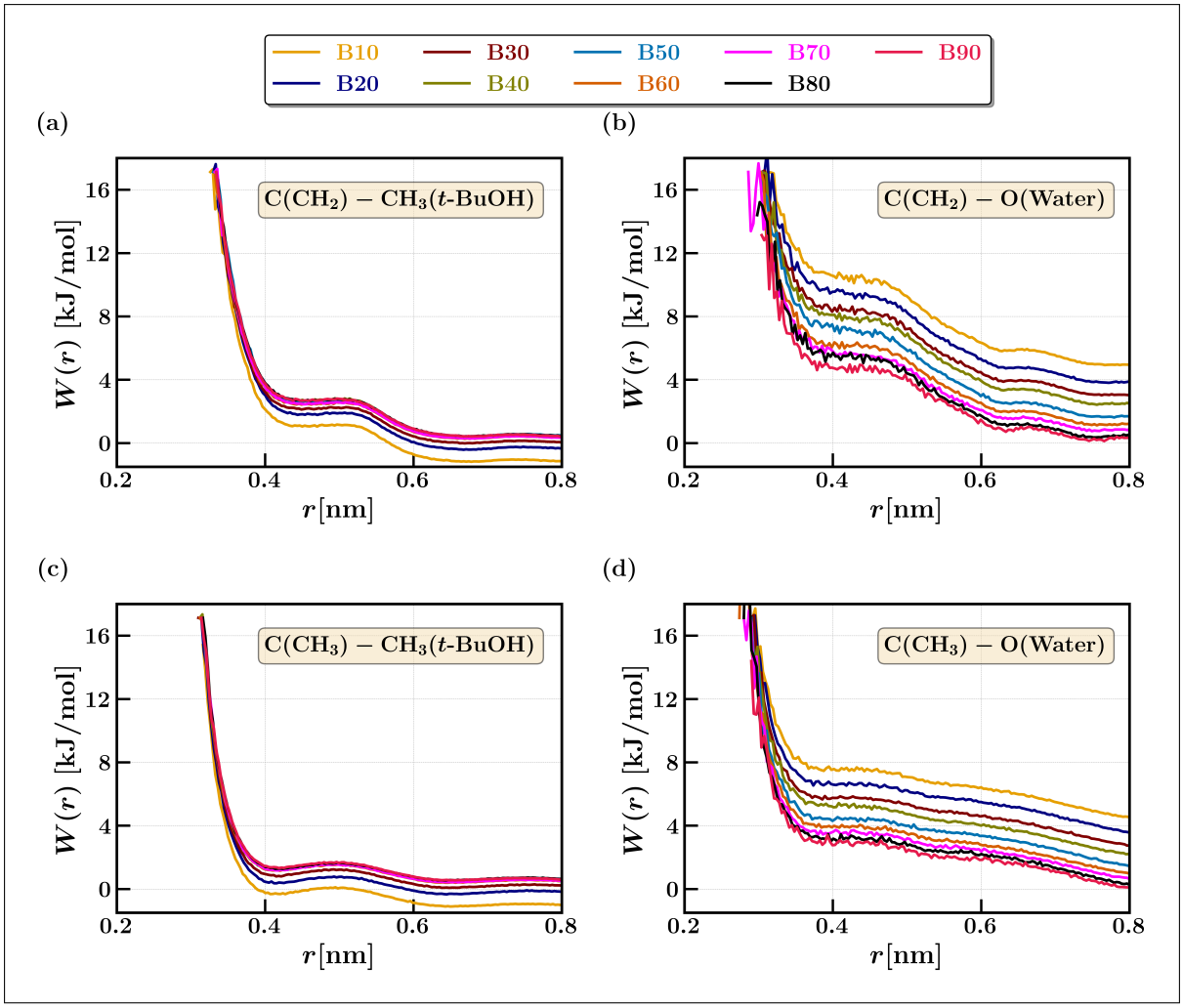

Figure S4: Potential of mean force, $W(r)$, between selected atom pairs of PMMA and water or *t*-BuOH at varying solvent mixing ratios. The notation "B" denotes *t*-BuOH, with the accompanying number indicating its mole fraction in the mixture (e.g., B10 corresponds to a 10 mol% *t*-BuOH solution).

The potential of mean force (PMF) analysis reveals that the interaction of *t*-BuOH with the nonpolar moieties of PMMA—specifically, the pendant CH_3 and backbone CH_2 groups—is energetically more favorable compared to water. This indicates that water exhibits stronger hydrophobic interactions with these nonpolar sites than *t*-BuOH, highlighting the preferential affinity of *t*-BuOH toward the nonpolar segments of PMMA.

Table S1: Energy comparison of optimized geometries for various PMMA configurations

Chain length, n	**Cis Energy,** E_{cis} **(kcal/mol)**	**Trans Energy,** E_{trans} **(kcal/mol)**	**Energy difference,** $E_{\text{cis}} - E_{\text{trans}}$ **(kcal/mol)**
Dimer ($n = 2$)	-434865.92	-434868.82	2.90
Tetramer ($n = 4$)	-868963.01	-868971.41	8.40

The table displays the energy values obtained through B3LYP/6-311G(d,p) calculations for different PMMA configurations. A comparison of the cis (isotactic) and trans (syndiotactic) configurations reveals that the trans-configuration is notably more stable.

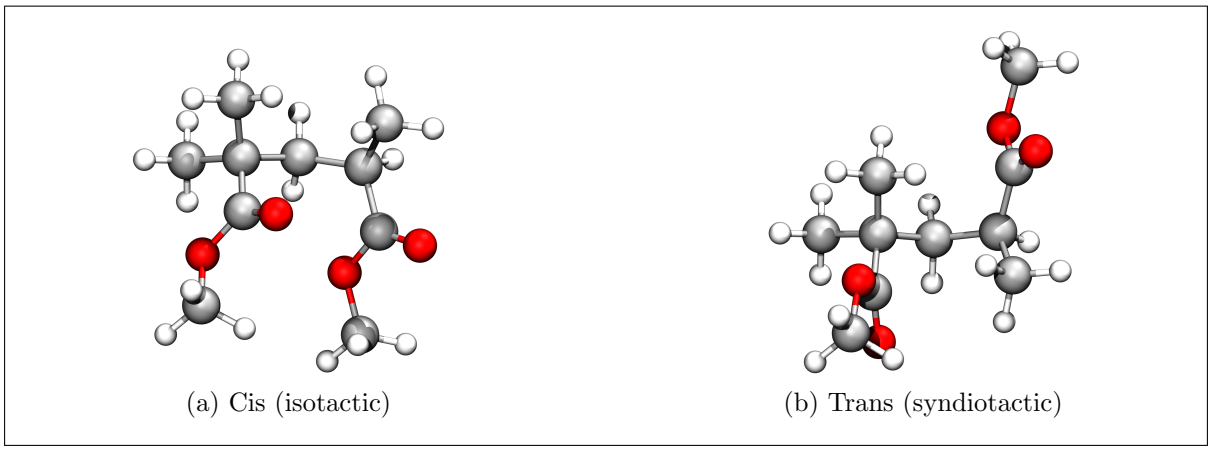

(a) Cis (isotactic) (b) Trans (syndiotactic)

Figure S5: Molecular structure of polymethyl-methacrylate (PMMA) dimer: (a) Cis (isotactic) and (b) Trans (syndiotactic) configuration.

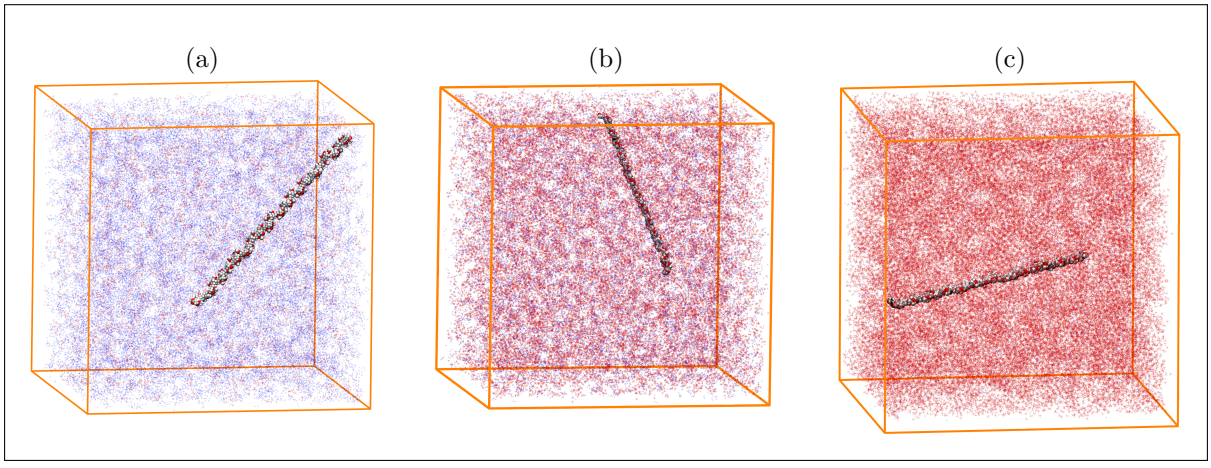

Figure S6: The snapshots of the initial simulation boxes for different compositions – (A) 10, (B) 50, and (C) 90 mole% of *tert*-butanol in the binary mixture of water and *tert*-butanol. In this illustration, vdw representation, red lines and blue lines are utilized to represent PMMA, *tert*-butanol, and water, respectively.

Table S2: Radius of gyration (R_g) of PMMA polymer chains in aqueous *tert*-butanol binary mixture. The solvent compositions are expressed as the mole fraction of *tert*-butanol ($x_{t\text{-BuOH}}$). The correlation length (ξ) of PMMA chains are compared relative to the (cubic) simulation box length. The reported values represent the largest R_g of PMMA in each system.

Mole fraction, $x_{t\text{-BuOH}}$	**Maximum** R_g **(nm)**	**Correlation length,** ξ **where** $R_g = \sqrt{3}\xi$ **(nm)**	**Simulation box length (nm)**	
			Initial	**Production run**
0	1.54	0.89	33.50	11.53
10	2.42	1.40	24.50	13.06
20	3.18	1.84	24.50	14.37
30	2.69	1.55	32.50	15.50
40	3.70	2.13	31.50	16.49
50	3.63	2.09	31.50	17.40
60	3.48	2.01	30.50	18.24
70	3.80	2.19	25.50	18.98
80	4.01	2.32	25.50	19.72
90	3.46	2.00	25.50	20.41
100	3.81	2.20	25.50	21.05